© 2018. Published by The Company of Biologists Ltd | Journal of Cell Science (2018) 131, jcs217083. doi:10.1242/jcs.217083

RESEARCH ARTICLE

PAI1 blocks NMDA receptor-mediated effects of tissue-type plasminogen activator on cell signaling and physiology

Steven L. Gonias[1,*], Michael A. Banki[1], Andrew S. Gilder[1], Pardis Azmoon[1], Wendy M. Campana[2] and Elisabetta Mantuano[1,3]

ABSTRACT

The fibrinolysis proteinase tissue-type plasminogen activator (tPA, also known as PLAT) triggers cell signaling and regulates cell physiology. In PC12 cells, Schwann cells and macrophages, the N-methyl-D-aspartate receptor (NMDA-R) mediates tPA signaling. Plasminogen activator inhibitor-1 (PAI1, also known as SERPINE1) is a rapidly acting inhibitor of tPA enzyme activity. Although tPA-initiated cell signaling is not dependent on its enzyme active site, we show that tPA signaling is neutralized by PAI1. In PC12 cells, PAI1 blocked the ERK1/2 activation mediated by tPA as well as neurite outgrowth. In Schwann cells, PAI1 blocked tPA-mediated ERK1/2 activation and cell migration. In macrophages, PAI1 blocked the ability of tPA to inhibit IκBα phosphorylation and cytokine expression. The cell signaling activity of tPA–PAI1 complex was rescued when the complex was formed with PAI1R^{76E}, which binds to LRP1 with decreased affinity, by pre-treating cells with the LRP1 antagonist receptor-associated protein and upon *LRP1* gene silencing. The inhibitory role of LRP1 in tPA–PAI1 complex-initiated cell signaling was unanticipated given the reported role of LRP1 as an NMDA-R co-receptor in signaling responses elicited by free tPA or α_2-macroglobulin. We conclude that PAI1 functions as an inhibitor not only of the enzyme activity of tPA but also of tPA receptor-mediated activities.

KEY WORDS: Tissue-type plasminogen activator, Plasminogen activator inhibitor-1, NMDA receptor, LDL receptor-related protein-1, LRP1, Fibrinolysis, Cell signaling

INTRODUCTION

Tissue-type plasminogen activator (tPA) is a serine proteinase and the major intravascular activator of fibrinolysis (Collen and Lijnen, 1991; Mosesson, 2005; Carmeliet et al., 1994). The structure of tPA includes a fibronectin type I/finger domain, an epidermal growth factor-like domain, two kringle domains and the serine proteinase module, which are encoded by distinct exons in the *PLAT* gene (Ny et al., 1984; Bode and Renatus, 1997). The multidomain structure of tPA is critical for interactions with fibrin, extracellular matrix proteins and cell surface receptors, which increase the catalytic efficiency of plasminogen activation and control localization of plasmin within tissues (van Zonneveld et al., 1986; Hoylaerts et al., 1982; Moser et al., 1993; Hajjar et al., 1994; Miles et al., 2014). tPA binding to extracellular matrix and cell surface proteins is also important for generating plasmin at sites where it is protected from its main inhibitors, α_2-antiplasmin and α_2-macroglobulin (α_2M) (Plow et al., 1986; Hall et al., 1991).

Through mechanisms that remain incompletely understood, tPA initiates cell signaling and regulates cell physiology. In neurons, the N-methyl-D-aspartate receptor (NMDA-R) functions as an essential component of a pathway by which tPA regulates cell survival and synaptic activity (Nicole et al., 2001; Wu et al., 2013; Yepes, 2015; Chevilley et al., 2015; Lesept et al., 2016; Jeanneret and Yepes, 2017; Liot et al., 2006). Because tPA binds to an ectodomain in the NMDA-R GluN1/NR1 (also known as GRIN1) subunit (Nicole et al., 2001; Lesept et al., 2016), the NMDA-R probably represents a true cell signaling receptor for tPA in neurons. The NMDA-R also functions as a tPA receptor in cells other than neurons, including macrophages and Schwann cells (SCs) (Mantuano et al., 2017, 2015). In macrophages, tPA-activated cell signaling suppresses innate immunity (Mantuano et al., 2017). In SCs, tPA promotes cell migration (Mantuano et al., 2015). tPA binding to the NMDA-R regulates the contractility of pulmonary arterial rings, suggesting that vascular smooth muscle cells respond to tPA (Nassar et al., 2011). In SCs, macrophages and PC12 cells, enzymatically active tPA (EA-tPA; wild-type protein) and enzymatically inactive tPA (EI-tPA; tPA with a S478A mutation, see Materials and Methods) demonstrate equivalent signaling activity, suggesting that domains other than the tPA serine proteinase module are involved (Mantuano et al., 2017, 2015, 2013). In support of this hypothesis, Parcq et al. (2013) identified an amino acid mutation in the Kringle-2 domain of tPA, which nullifies NMDA-R-mediated activities in cortical neurons.

When tPA initiates cell signaling, LDL receptor-related protein-1 (LRP1) apparently functions as a NMDA-R co-receptor (Yepes, 2015; Mantuano et al., 2015, 2013; Samson et al., 2008; Echeverry et al., 2010). tPA binds directly to the extracellular α-chain of LRP1 (Bu et al., 1992). In PC-12 cells, N2a cells and SCs, the LRP1 antagonist, receptor-associated protein (RAP, also known as LRPAP1), does not block tPA signaling; however, the concentration of tPA required to observe cell signaling is increased (Mantuano et al., 2015, 2013). It is possible that tPA bridges LRP1 to the NMDA-R to effectively trigger cell signaling. LRP1 and the NMDA-R also may be bridged on the intracellular side of the plasma membrane by the bi-functional adaptor protein PSD-95 (also known as DLG4) (Mantuano et al., 2013; May et al., 2004; Martin et al., 2008; Nakajima et al., 2013). Other LRP1 ligands, such as α_2M, trigger cell signaling in an NMDA-R-dependent manner; however, unlike tPA, α_2M appears to have an absolute requirement for LRP1 in order to signal (Mantuano et al., 2013, 2015; Bacskai et al., 2000; Qiu et al., 2002).

Plasminogen activator inhibitor-1 (PAI1, also known as SERPINE1) is a member of the Serpin gene family and a rapid

[1]Department of Pathology, University of California San Diego, La Jolla CA 92093, USA. [2]Department of Anesthesiology and the Program in Neuroscience, University of California San Diego, La Jolla CA 92093, USA. [3]Department of Experimental Medicine, Sapienza University of Rome, 00161 Rome, Italy.

*Author for correspondence (sgonias@ucsd.edu)

S.L.G., 0000-0003-0843-4607

Received 21 February 2018; Accepted 29 May 2018

Journal of Cell Science (2018) 131, jcs217083. doi:10.1242/jcs.217083

inhibitor of both tPA and urokinase-type plasminogen activator (uPA; also known as PLAU) (Hekman and Loskutoff, 1988). When tPA or uPA bind to PAI1, the complex binds to LRP1 with increased affinity (K_D of 5-10 nM), reflecting the unmasking of a nascent LRP1-binding site in PAI1 (Herz et al., 1992; Orth et al., 1992; Stefansson et al., 1998). PAI1 has diverse effects on cell physiology, some of which are unrelated to its role as an inhibitor of tPA and uPA. For example, binding of PAI1 to vitronectin regulates cell adhesion mediated by integrins and the urokinase receptor (uPAR) (Stefansson and Lawrence, 1996; Czekay et al., 2003; Deng et al., 1996). In cancer cells, PAI1 alters the cell signaling response triggered by uPA, so that uPA is converted into a cancer cell mitogen (Webb et al., 2001). When the PAI1 gene is deleted in mice, cancer invasion and angiogenesis are inhibited (Bajou et al., 1998). Furthermore, in at least seven different types of human malignancy, high PAI1 expression is associated with an unfavorable prognosis, as determined by analysis of datasets of The Cancer Genome Atlas, summarized in the Protein Atlas (Uhlen et al., 2017). Plasma PAI1 levels are increased in conditions associated with inflammation, including metabolic syndrome, cardiovascular disease and diabetes (De Taeye et al., 2005; Devaraj et al., 2003; Alessi and Juhan-Vague, 2006).

In the present study, we examined the effects of PAI1 on tPA-initiated cell signaling in three separate cell types. In all three model systems, PAI1 neutralized the signaling activity of tPA. In macrophages, PAI1 blocked the anti-inflammatory activity of tPA. In PC12 cells, PAI1 blocked the effects of tPA on neurite outgrowth, and in SCs, PAI1 inhibited tPA-induced cell migration. Mechanistically, the ability of PAI1 to block tPA signaling required LRP1. Accordingly, the cell signaling activity of tPA–PAI1 complex was rescued using three separate approaches: (1) upon forming a tPA–PAI1 complex with mutated PAI1 ($PAI1^{R76E}$), which binds to LRP1 with greatly decreased affinity (Stefansson et al., 1998); (2) upon treating cells with tPA–PAI1 complex in the presence of RAP; and (3) upon silencing *LRP1* gene expression. Our results demonstrate that PAI1 functions not only as an inhibitor of the enzymatic activity of tPA but also as a regulator of receptor-mediated tPA activities.

RESULTS

PAI1 neutralizes the effects of EA-tPA on PC12 cell signaling and neurite outgrowth

To begin, we studied human PAI1, which is mutated to enhance stability and expressed in *E. coli* and thus not glycosylated. To confirm that the PAI1 was active, we incubated EA-tPA with an equimolar concentration of PAI1 or a 3-fold molar excess of PAI1 for 30 min. tPA activity was assessed in a coupled enzyme assay with purified human plasminogen and the plasmin-specific substrate H-D-Val-Leu-Lys-p-nitroanilide (S-2251). In the absence of PAI1, time-dependent plasminogen activation and S-2251 hydrolysis were observed (Fig. 1A). PAI1 at both concentrations completely neutralized plasminogen activation, indicating complex formation. Equivalent results were obtained when EA-tPA was pre-incubated with glycosylated PAI1 (gPAI1) expressed in insect cells or with $PAI1^{R76E}$ (Stefansson et al., 1998) (results not shown). Unless otherwise stated, tPA–PAI1 complexes were formed using a 3-fold molar excess of PAI1.

In PC12 cells, tPA activates ERK1 and ERK2 (ERK1/2, also known as MAPK3 and MAPK1, respectively) through a pathway that requires the NMDA-R (Mantuano et al., 2013). We treated PC12 cells for 10 min with increasing concentrations of EA-tPA or preformed EA-tPA–PAI1 complex (12–100 nM). EA-tPA, at each concentration studied, activated ERK1/2 (Fig. 1B). EA-tPA–PAI1 complex failed to activate ERK1/2 at the equivalent concentrations. Free PAI1 (36 nM) also failed to activate ERK1/2.

EI-tPA and EA-tPA activate ERK1/2 in PC12 cells equivalently, suggesting that the enzyme active site of tPA is not involved (Mantuano et al., 2013). To confirm that PAI1 does not block the signaling activity of EA-tPA by neutralizing its enzymatic activity, we treated EA-tPA with the irreversible active site inhibitor 4-(2-aminoethyl) benzene sulfonyl fluoride HCl (AEBSF) (1.0 mM) for 2 h. Complete neutralization of the enzymatic activity of EA-tPA was confirmed in coupled enzyme assays with plasminogen and S-2251 (results not shown). Free AEBSF was removed by extensive dialysis. AEBSF-treated EA-tPA activated ERK1/2 equivalently to non-treated EA-tPA (Fig. 1C). Free AEBSF (10 µM) did not activate ERK1/2.

To test the role of the NMDA-R in tPA signaling in PC12 cells, cells were treated with the non-competitive NMDA-R antagonist MK801. ERK1/2 activation in response to EA-tPA was blocked (Fig. 1D), as anticipated (Mantuano et al., 2013). EA-tPA–PAI1 complex failed to trigger cell signaling in MK801-treated PC12 cells and in cells that were not treated with MK801.

Next, we studied PC12 cell neurite outgrowth, a process that requires ERK1/2 activation (Vaudry et al., 2002). Cells were treated with EA-tPA (12 nM), EI-tPA (12 nM), preformed EA-tPA–PAI1 complex (12 nM), free PAI1 (36 nM) or nerve growth factor-β (NGFβ) (50 ng/ml), as a positive control. Neurite outgrowth was allowed to occur for 48 h in serum-free medium (SFM). Representative images are shown in Fig. 1E, and the results of four separate experiments are summarized in Fig. 1F. Mean neurite length was significantly increased by both EA-tPA and EI-tPA. The responses observed with EA-tPA and EI-tPA were similar in magnitude to those observed with NGFβ. Preformed EA-tPA–PAI1 complex failed to promote neurite outgrowth. Free PAI1 (36 nM) was also inactive.

PAI1 blocks the effects of EA-tPA on SC signaling and cell migration

EI-tPA activates cell signaling in SCs and the response requires the NMDA-R (Mantuano et al., 2015). Fig. 2A shows that EA-tPA (12 nM) activated ERK1/2 in SCs. The response was evident at 10 min and sustained through 60 min. By contrast, preformed EA-tPA–PAI1 complex (12 nM) failed to activate ERK1/2. Free PAI1 (36 nM) also was inactive. MK801 inhibited ERK1/2 activation mediated by EA-tPA (Fig. 2B), confirming an essential role for the NMDA-R (Mantuano et al., 2015).

ERK1/2 activation in SCs is typically associated with increased cell migration (Mantuano et al., 2008, 2010, 2015). We therefore treated SCs with EA-tPA (12 nM), free PAI1 (36 nM) or preformed EA-tPA–PAI1 complex (12 nM), and tested whether cell migration was regulated by allowing the cells to migrate in Transwell chambers for 4 h. Representative images of the underside surfaces of membranes are shown in Fig. 2C, and the results of four separate experiments are summarized in Fig. 2D. EA-tPA stimulated SC migration more than 4-fold. By contrast, preformed EA-tPA–PAI1 complex and free PAI1 had no effect on SC migration.

PAI1 neutralizes the effects of EA-tPA on the response to LPS in macrophages

We previously demonstrated that EI-tPA and EA-tPA inhibit the ability of lipopolysaccharide (LPS) to induce sustained IκBα phosphorylation and cytokine expression in bone marrow-derived macrophages (BMDMs) (Mantuano et al., 2016, 2017). Using equivalent methods, we compared the effects of free EA-tPA and

Journal of Cell Science (2018) 131, jcs217083. doi:10.1242/jcs.217083

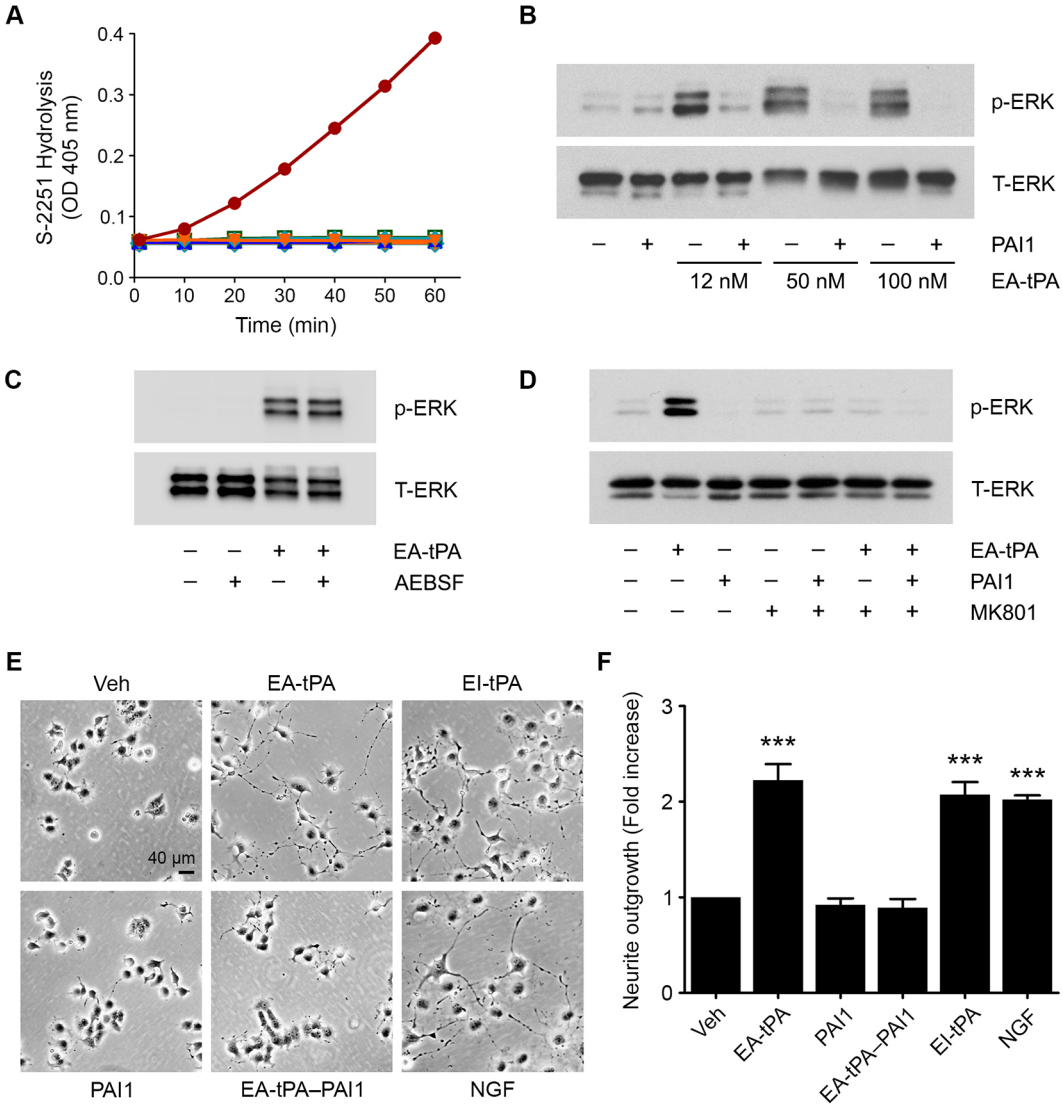

Fig. 1. PAI1 blocks ERK1/2 activation and neurite outgrowth induced by EA-tPA in PC12 cells. (A) The following proteins were incubated with S-2251 (0.2 mM): plasminogen (0.2 µM) (black star); PAI1 (12 nM) (open green square); PAI1 (36 nM) (open blue triangle); EA-tPA (12 nM) (open red circle); EA-tPA–PAI1 complex formed with an equimolar concentration of EA-tPA and PAI1 (12 nM) (open teal diamond); EA-tPA–PAI1 complex formed with a 3-fold molar excess of PAI1 (12 nM EA-tPA) (open orange inverted triangle); PAI1 (12 nM) plus plasminogen (0.2 µM) (closed green square); PAI1 (36 nM) plus plasminogen (0.2 µM) (closed blue triangle); EA-tPA (12 nM) plus plasminogen (0.2 µM) (closed red circle); EA-tPA–PAI1 complex formed with an equimolar concentration of EA-tPA and PAI1 plus plasminogen (0.2 µM) (closed teal diamond); and EA-tPA–PAI1 complex formed with a 3-fold molar excess of PAI1 plus plasminogen (0.2 µM) (closed orange inverted triangle). The absorbance at 405 nm was determined every 10 min for 1 h. Not all results can be distinguished owing to their similarity, except EA-tPA plus plasminogen. (B) PC12 cells were serum starved for 4 h and then treated with increasing concentrations of EA-tPA (12–100 nM) or preformed EA-tPA–PAI1 complex for 10 min. Additional cultures were treated with free PAI1 (36 nM) or vehicle. Equal amounts of cellular protein (10 µg) were subjected to SDS-PAGE. Immunoblot analysis was performed to detect phosphorylated ERK1/2 (p-ERK) and total ERK1/2 (T-ERK). (C) EA-tPA was treated with AEBSF (1 mM) for 3 h and then subjected to 1:2500 (vol/vol) dialysis. PC12 cells were treated with EA-tPA (12 nM), AEBSF-inactivated EA-tPA (12 nM), free AEBSF (10 µM) or vehicle for 10 min. Immunoblot analysis was performed to detect p-ERK1/2 and T-ERK1/2. (D) PC12 cells were pre-treated with MK801 (1 µM) or vehicle and then with free PAI1 (36 nM), EA-tPA (12 nM), preformed EA-tPA-PAI1 complex (12 nM) or vehicle for 10 min. Immunoblot analysis was performed to detect p-ERK1/2 and T-ERK1/2. (E) PC12 cells were treated with EA-tPA (12 nM), EI-tPA (12 nM), PAI1 (36 nM), preformed EA-tPA–PAI1 complex (12 nM), NGFβ (50 ng/ml) or vehicle (Veh) for 48 h. Neurite outgrowth was assessed by phase-contrast microscopy. Representative images are shown. Scale bar: 40 µm. (F) Neurite outgrowth results were quantified. Neurite length was determined using ImageJ. Data are expressed as the mean±s.e.m. (n=4, ***P<0.001 compared with the vehicle control; one-way ANOVA and Dunnett's test).

preformed EA-tPA–PAI1 complex. Fig. 3A shows that the treatment of BMDMs with LPS (0.1 µg/ml) for 1 h induced phosphorylation of IκBα (encoded by *NFKBIA*) and a decrease in the total abundance of IκBα. These events report NFκB activation (Ghosh and Karin, 2002).

When BMDMs were treated with LPS together with EA-tPA (12–24 nM), IκBα phosphorylation and the decrease in total IκBα were blocked. By contrast, EA-tPA–PAI1 complex (0.2–24 nM) failed to reverse the effects of LPS on IκBα phosphorylation and abundance. Free PAI1 (72 nM) also had no effect. In the absence of LPS, EA-tPA–PAI1 complex (24 nM) did not cause IκBα phosphorylation.

Next, BMDMs were treated with LPS (0.1 µg/ml), EA-tPA (12 nM) or EA-tPA–PAI1 complex (12 nM), alone or in combination. After 6 h, expression of pro-inflammatory cytokines was determined by real-time quantitative PCR (RT-qPCR). In the

Journal of Cell Science (2018) 131, jcs217083. doi:10.1242/jcs.217083

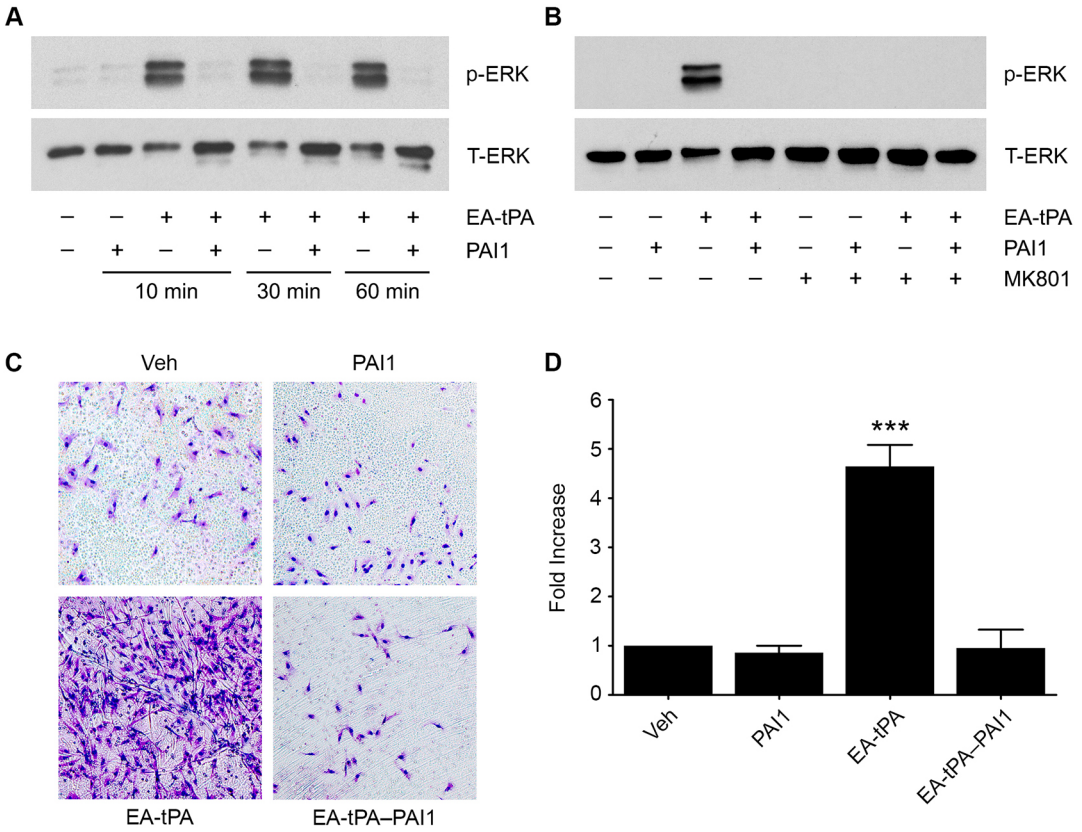

Fig. 2. PAI1 blocks ERK1/2 activation and cell migration induced by EA-tPA in SCs. (A) Primary cultures of SCs were serum-starved for 1 h and then treated with free PAI1 (36 nM), EA-tPA (12 nM), preformed EA-tPA–PAI1 complex (12 nM) or vehicle (Veh) for various times up to 1 h. Immunoblot analysis was performed to detect phosphorylated ERK1/2 (p-ERK) and total ERK1/2 (T-ERK). (B) SCs were pre-treated with MK801 (1 µM) or with vehicle for 30 min and then with PAI1 (36 nM), EA-tPA (12 nM), preformed EA-tPA–PAI1 complex (12 nM) or vehicle for 10 min. Cell extracts were subject to immunoblot analysis to detect p-ERK1/2 and T-ERK1/2. (C) SCs were treated with PAI1 (36 nM), EA-tPA (12 nM), preformed EA-tPA–PAI1 complex (12 nM) or vehicle. SC migration was studied. Migration was allowed to proceed for 4 h at 37°C. Representative images of SCs that migrated across Transwell membranes to the lower membrane surfaces are shown. (D) Quantification of cell migration results. Data are expressed as the mean±s.e.m. (n=4, ***P<0.001 compared with the vehicle control; one-way ANOVA and Dunnett's test).

absence of other reagents, LPS induced expression of the mRNAs encoding tumor necrosis factor (TNF), chemokine C-C motif ligand 3 (CCL3), interleukin-1β (IL-1β) and interleukin-6 (IL-6) (Fig. 3B). EA-tPA blocked cytokine expression in response to LPS, as anticipated (Mantuano et al., 2017). By contrast, EA-tPA–PAI1 complex failed to block LPS-induced cytokine expression.

gPAI1 behaves equivalently to PAI1 expressed in bacteria

The results presented thus far suggest that when EA-tPA binds PAI1, the PAI1 disallows a key interaction required for initiation of cell signaling and regulation of cell physiology by tPA. To determine whether this PAI1 activity is unique to the non-glycosylated form of the Serpin, we examined cell signaling in response to EA-tPA–PAI1 complex formed with gPAI1, expressed in insect cells. EA-tPA–gPAI1 complex failed to activate ERK1/2 in PC12 cells (Fig. 4A). EA-tPA–gPAI complex also failed to activate ERK1/2 in SCs (Fig. 4B). In both studies, free EA-tPA demonstrated the anticipated cell signaling activity.

PAI1 does not neutralize the cell signaling activity of EI-tPA

In EI-tPA, mutation of the active site serine (S478A) blocks the principal interaction that leads to irreversible complex formation between tPA and PAI1 (Hekman and Loskutoff, 1988). We therefore performed studies to test whether PAI1 antagonizes the cell signaling activity of EI-tPA. EI-tPA was incubated with a 3-fold molar excess of PAI1 for 30 min. PC12 cells were treated with this preparation (12 nM EI-tPA, 36 nM PAI1) for 10 min or with EI-tPA (12 nM), EA-tPA (12 nM), preformed EA-tPA–PAI1 complex (12 nM) or free PAI1 (36 nM). Fig. 5A shows that both EA-tPA and EI-tPA activated ERK1/2 in PC12 cells, as anticipated (Mantuano et al., 2013). EA-tPA–PAI1 complex failed to activate ERK1/2. By contrast, EI-tPA that was pre-incubated with a 3-fold molar excess of PAI1 demonstrated unchanged activity, inducing ERK1/2 phosphorylation to the same extent as EI-tPA that was not exposed to PAI1.

Next, we examined SCs. EI-tPA (12 nM) activated ERK1/2 in SCs and pre-incubating EI-tPA (12 nM) with PAI1 (36 nM) for 30 min failed to inhibit the cell signaling activity of the EI-tPA (Fig. 5B). In cell migration studies, EI-tPA (12 nM) and EI-tPA (12 nM) that was pre-incubated with PAI1 (36 nM) for 30 min demonstrated equivalent activity, increasing SC migration by ∼4-fold (Fig. 5C,D). Free PAI1 failed to stimulate SC migration.

Blocking the interaction of EA-tPA–PAI1 complex with LRP1 rescues its cell signaling activity

EA-tPA–PAI1 complex was formed with PAI1^{R76E}. This complex binds to LRP1 with substantially decreased affinity compared with EA-tPA–PAI1 complex formed with wild-type PAI1 (Stefansson et al., 1998). EA-tPA–PAI1^{R76E} complex (12 nM) activated ERK1/2 in PC12 cells and the magnitude of the response

Journal of Cell Science (2018) 131, jcs217083. doi:10.1242/jcs.217083

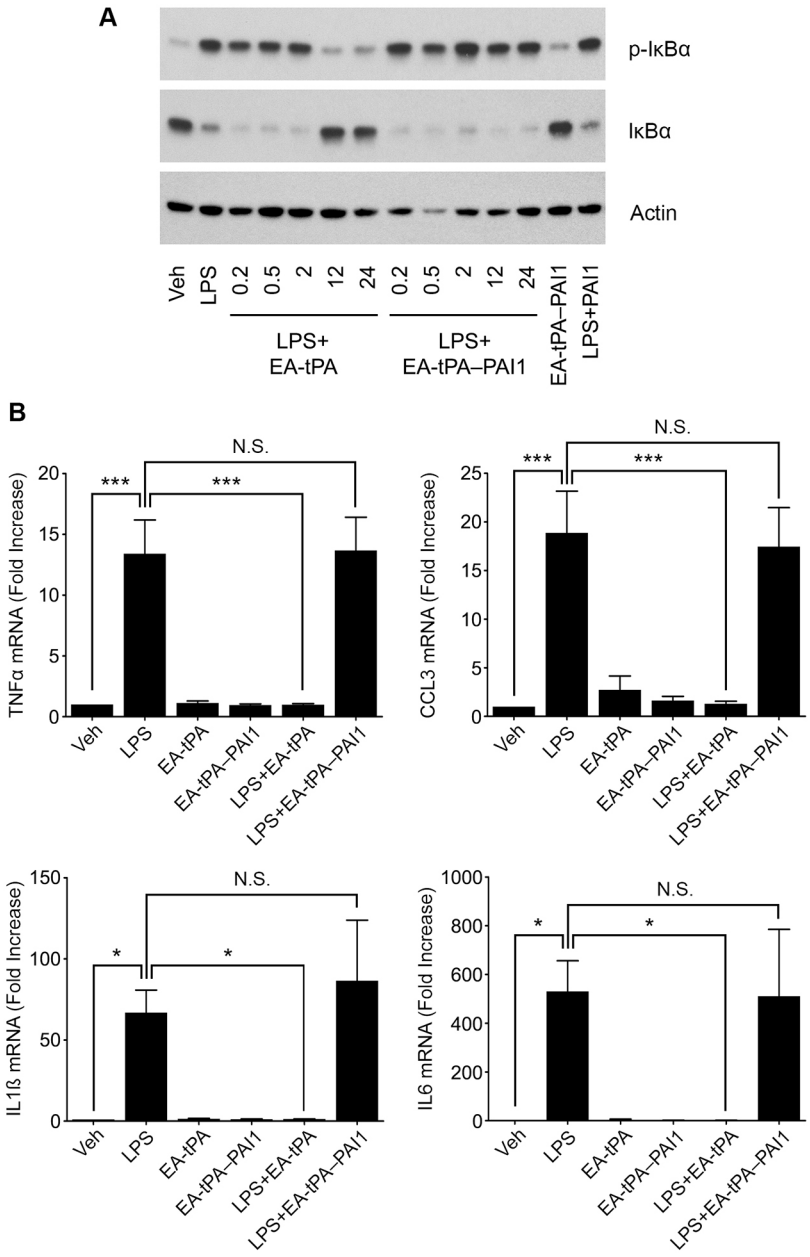

Fig. 3. PAI1 neutralizes the ability of EA-tPA to counteract the effects of LPS in BMDMs. (A) BMDMs from C57BL/6J mice were treated with LPS (0.1 µg/ml), LPS (0.1 µg/ml) plus EA-tPA (0.2–24 nM), LPS (0.1 µg/ml) plus preformed EA-tPA–PAI1 complex (0.2–24 nM), preformed EA-tPA–PAI1 complex (24 nM) in the absence of LPS, LPS (0.1 µg/ml) plus free PAI1 (36 nM), or vehicle (Veh) for 1 h. Immunoblot analysis was performed to detect phosphorylated IκBα (p-IκBα) and total IκBα. Blots were re-probed for β-actin as a control for load. (B) BMDMs were treated with LPS (0.1 µg/ml), EA-tPA (12 nM), preformed EA-tPA–PAI1 complex (12 nM), LPS (0.1 µg/ml) plus EA-tPA (12 nM), LPS (0.1 µg/ml) plus preformed EA-tPA–PAI1 complex (12 nM) or vehicle for 6 h. Expression of the mRNAs encoding TNF (TNFα), CCL3, IL-1β and IL-6 was determined (mean±s.e.m.; n=5; *P<0.05, ***P<0.001, N.S., not statistically significant; one-way ANOVA with Tukey's post hoc test).

was equivalent to that observed with free EA-tPA (12 nM) (Fig. 6A).

Next, we pre-treated PC12 cells with 150 nM RAP for 30 min before introducing EA-tPA–PAI1 complex formed with wild-type PAI1. RAP binds to the ligand-binding domains of LRP1 and inhibits binding of other ligands (Williams et al., 1992). In PC12 cells pre-treated with RAP, EA-tPA–PAI1 complex formed with wild-type PAI1 (12 nM) activated ERK1/2 (Fig. 6B). EA-tPA–PAI1^{R76E} complex activated ERK1/2 in the presence or absence of RAP.

Finally, we silenced *LRP1* gene expression in PC12 cells, using our established method (Mantuano et al., 2013). Control cells were transfected with non-targeting control (NTC) siRNA. *LRP1* gene silencing resulted in a 72±3% (mean±s.d.) decrease in LRP1 protein as determined by immunoblot analysis (Fig. 6C) and densitometry. In LRP1 gene-silenced cells, 12 nM of EA-tPA–PAI1 complex, formed with wild-type PAI1, activated ERK1/2 comparably to EA-tPA. In control cells transfected with NTC siRNA, ERK1/2 activation was observed in response to EA-tPA but not EA-tPA–PAI1 complex. Collectively, these results demonstrate that LRP1 inhibits the cell signaling activity of EA-tPA–PAI1 complex.

EA-tPA and EA-tPA-PAI1 complex bind to immunopurified NMDA-R

We coupled NMDA-R NR1 subunit-specific antibody (NR1-Ab) to Protein G–Dynabeads and immunopurified NMDA-R from extracts of mouse cortex. As a control, we coupled non-specific IgG (NS-IgG) to Protein G–Dynabeads and incubated these beads with the equivalent mouse cortical extracts. Immunoblot analysis for NR1 confirmed that NMDA-R was recovered selectively in association with anti-NR1 antibody but not NS-IgG (Fig. 7A).

NR1-Ab and NS-IgG were 'pre-loaded' with NMDA-R by incubation with mouse cortical extracts, washed and then incubated with ^{125}I-EA-tPA (12 nM). Binding of ^{125}I-EA-tPA to pre-loaded NR1-Ab was significantly increased compared with its binding to pre-loaded NS-IgG (P<0.01; n=6, unpaired

Journal of Cell Science (2018) 131, jcs217083. doi:10.1242/jcs.217083

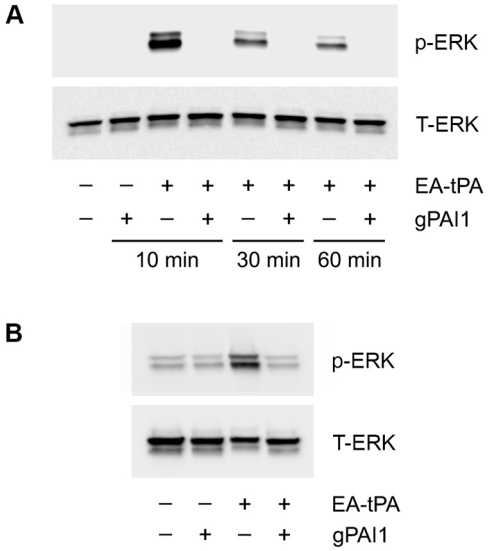

Fig. 4. Glycosylated PAI1 blocks EA-tPA-initiated cell signaling. (A) PC12 cells were treated with gPAI1 (36 nM), EA-tPA (12 nM), preformed EA-tPA–gPAI1 complex (12 nM) or vehicle for the indicated times. Immunoblot analysis was performed to detect phosphorylated ERK1/2 (p-ERK) and total ERK1/2 (T-ERK). (B) SCs were treated with gPAI1 (36 nM), EA-tPA (12 nM), EA-tPA–gPAI1 complex (12 nM) or vehicle for 10 min. Immunoblot analysis was performed to detect p-ERK1/2 and T-ERK1/2.

Student's *t*-test) (Fig. 7B). ^{125}I-tPA–PAI1 complex also bound at significantly increased levels to pre-loaded NR1-Ab compared with its binding to NS-IgG (P<0.01, n=6, unpaired Student's *t*-test) (Fig. 7C). When all four binding studies were analyzed collectively by ANOVA with a Tukey's post hoc test, it was found that binding of ^{125}I-tPA–PAI1 complex to pre-loaded NR1-Ab was significantly lower than that of ^{125}I-tPA (P<0.01).

To test whether the NMDA-R is required for activation of cell signaling by EA-tPA–PAI1 complex when LRP1 is neutralized, we treated PC12 cells with MK801 and then with EA-tPA–PAI1^{R76E} complex (12 nM). MK801 blocked ERK1/2 activation by EA-tPA–PAI1^{R76E} complex (Fig. 7D).

DISCUSSION

Elevated plasma PAI1 is associated with diverse diseases that have an important inflammatory component, including thrombo-atherosclerotic cardiovascular disease, metabolic syndrome and diabetes (De Taeye et al., 2005; Devaraj et al., 2003; Alessi and Juhan-Vague, 2006). Potent pro-inflammatory mediators such as LPS and TNF induce PAI1 expression in mice (Sawdey and Loskutoff, 1991). C-reactive protein, a biomarker of inflammation, increases PAI1 expression by endothelial cells in culture (Devaraj et al., 2003). It is thus well supported that PAI1 is increased in a variety of pathophysiologic states that involve inflammation. Whether PAI1 is a biomarker of inflammation or contributes actively to the process remains incompletely understood.

We previously identified a receptor-mediated pathway in macrophages by which tPA suppresses innate immunity and inflammation (Mantuano et al., 2016, 2017). This pathway requires NMDA-R (Mantuano et al., 2017), as does tPA-initiated cell signaling in SCs and PC12 cells (Mantuano et al., 2013, 2015). The results presented here and elsewhere (Mantuano et al., 2013, 2015, 2017) demonstrate that the enzyme activity of tPA is not required for activation of cell signaling via the NMDA-R. Nevertheless, when tPA forms a complex with PAI1, not only is the enzyme activity of EA-tPA neutralized, but also the ability of EA-tPA to trigger NMDA-R-dependent cell signaling. As a result, PAI1 reverses the activity of EA-tPA as a stimulant of neurite outgrowth in PC12 cells, as a stimulant of SC migration and as a suppressor of LPS-induced cytokine expression in BMDMs.

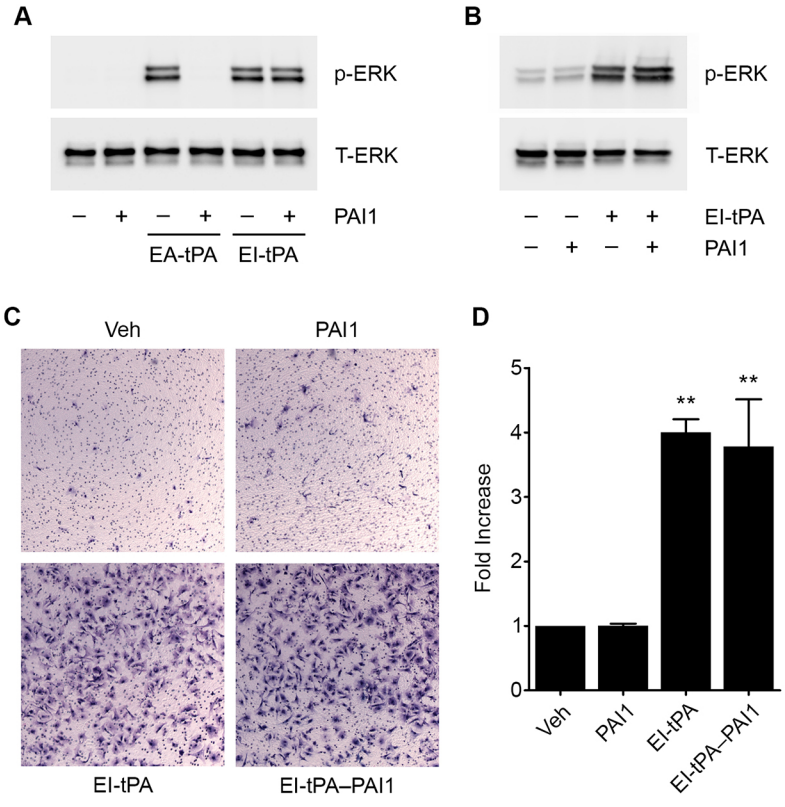

Fig. 5. The effects of EI-tPA on ERK1/2 activation and SC migration are not inhibited by PAI1. (A) PC12 cells were treated for 10 min with PAI1 (36 nM), EA-tPA (12 nM), EI-tPA (12 nM), preformed EA-tPA–PAI1 complex (12 nM), EI-tPA (12 nM) that was pre-incubated with 36 nM PAI1, or vehicle (Veh). Immunoblot analysis was performed to detect phosphorylated ERK1/2 (p-ERK) and total ERK1/2 (T-ERK). (B) SCs were treated for 10 min with free PAI1 (36 nM), EI-tPA (12 nM), EI-tPA (12 nM) that was pre-incubated with PAI1 (36 nM), or vehicle. Immunoblot analysis was performed to detect p-ERK1/2 and T-ERK1/2. (C) SCs were treated with PAI1 (36 nM), EI-tPA (12 nM), EI-tPA (12 nM) that was pre-incubated with PAI1 (36 nM), or vehicle. Migration was allowed to proceed for 4 h at 37°C. Representative images of SCs that migrated to the lower membrane surfaces are shown. (D) Quantification of cell migration results. Data are expressed as the mean±s.e.m. (n=4, **P<0.01 compared with the vehicle control; one-way ANOVA and Dunnett's test).

Journal of Cell Science (2018) 131, jcs217083. doi:10.1242/jcs.217083

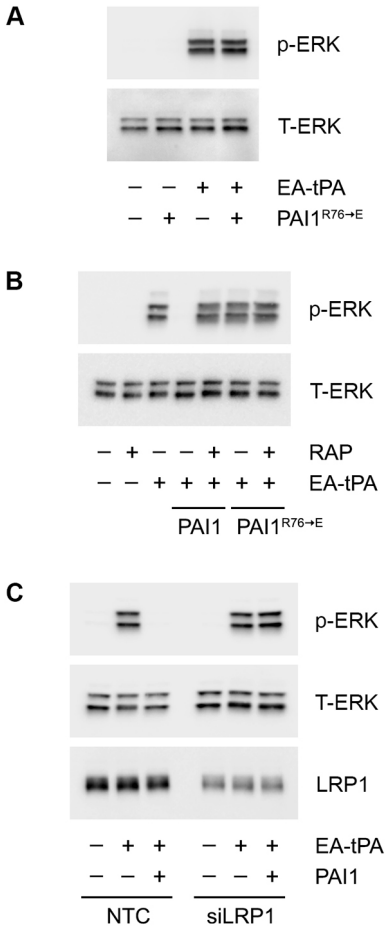

Fig. 6. Neutralizing LRP1 de-represses the signaling activity of EA-tPA–PAI1 complex. (A) PC12 cells were treated with PAI1^{R76E} (36 nM), EA-tPA (12 nM), preformed EA-tPA–PAI1^{R76E} complex (12 nM) or vehicle for 10 min. Immunoblot analysis was performed to detect phosphorylated ERK1/2 (p-ERK) and total ERK1/2 (T-ERK). (B) PC12 cells were pre-treated with RAP (150 nM) or vehicle for 30 min and then with PAI1 (36 nM), PAI1^{R76E} (36 nM), EA-tPA (12 nM), preformed EA-tPA–PAI1 complex (12 nM), preformed EA-tPA–PAI1^{R76E} complex (12 nM) or vehicle for 10 min. Cell extracts were subject to immunoblot analysis to detect p-ERK1/2 and T-ERK1/2. (C) PC12 cells in which *LRP1* was silenced and control cells, transfected with NTC siRNA, were treated with EA-tPA (12 nM), preformed EA-tPA–PAI1 complex (12 nM) or vehicle for 60 min. Immunoblot analysis was performed to detect p-ERK1/2, T-ERK1/2 and LRP1.

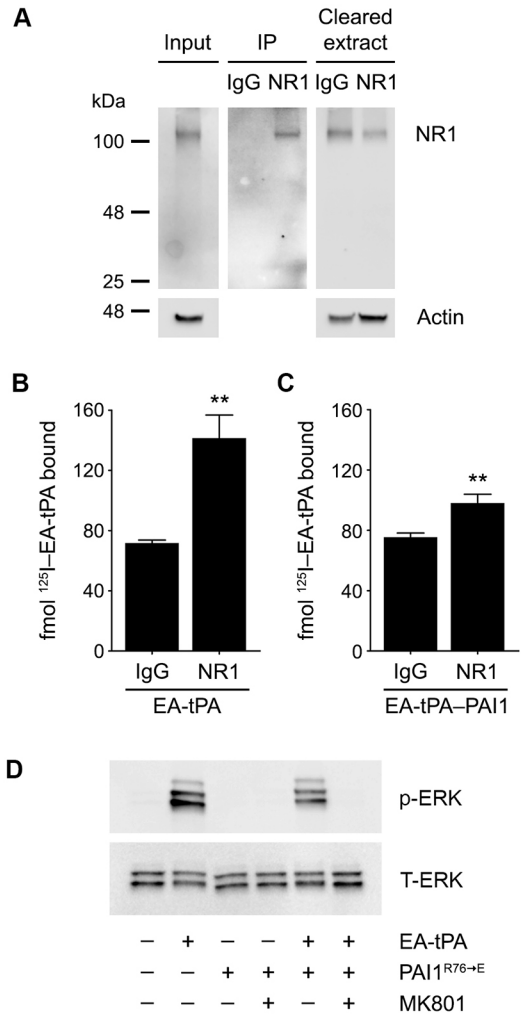

Fig. 7. PAI1 inhibits binding of EA-tPA to immunopurified NMDA-R. (A) Extracts of mouse cortex were incubated with NMDA-R NR1 subunit-specific antibody (NR1) or with NS-IgG (IgG) coupled to Protein-G–Dynabeads. Bound proteins were immunoprecipitated in an acidic solution, neutralized and subjected to immunoblot analysis to detect NMDA-R NR1 subunit (IP). As a control, the original extracts were subjected to immunoblot analysis to detect the NR1 subunit and actin prior to incubation with Protein-G–Dynabeads (input) and after immunoprecipitation (cleared extract). (B) NMDA-R NR1 subunit-specific antibody (NR1) or NS-IgG (IgG) coupled to Protein-G–Dynabeads were pre-incubated with mouse cortical extracts, washed extensively and incubated with ^{125}I-EA-tPA (12 nM) for 2 h at 4°C. The beads were washed extensively again. ^{125}I-EA-tPA that was associated with the Dynabeads was determined in a γ-irradiation counter (mean±s.e.m., n=6; $^{**}P$<0.01, unpaired t-test). (C) ^{125}I-EA-tPA–PAI1 complex was incubated with pre-loaded NMDA-R NR1 subunit-specific antibody (NR1) or NS-IgG (IgG) coupled to Protein-G–Dynabeads for 2 h at 4°C. The beads were washed. ^{125}I-EA-tPA–PAI1 complex that was associated with the Dynabeads was determined in a γ-irradiation counter (mean±s.e.m., n=6; $^{**}P$<0.01, unpaired t-test). (D) PC12 cells were pre-treated with MK801 (1 µM) or with vehicle for 30 min and then with EA-tPA (12 nM), EA-tPA–PAI1^{R76E} complex (12 nM) or vehicle for 10 min. The presence of phosphorylated ERK1/2 (p-ERK) and total ERK1/2 (T-ERK) were determined by immunoblot analysis.

Equivalent results were obtained with non-glycosylated PAI1 and with gPAI1. We conclude that PAI1 functions to neutralize the proteinase activity of tPA and various activities of tPA resulting from interaction with the NMDA-R.

In PC12 cells and SCs, LRP1 is not essential for tPA signaling; however, neutralizing the activity of LRP1 with RAP increases the concentration of tPA required to trigger a signaling response (Mantuano et al., 2013, 2015). Activation of cell signaling by α_2M requires both the NMDA-R and LRP1 in SCs and PC12 cells; α_2M-initiated cell signaling is blocked by RAP in these cells (Mantuano et al., 2013, 2015; Bacskai et al., 2000; Qiu et al., 2002). The function of LRP1 in regulating tPA–PAI1 complex-induced cell signaling is thus a new discovery. By using three distinct approaches, we demonstrate that LRP1 inhibits cell signaling by tPA–PAI1 complex. The signaling activity of tPA–PAI1 complex was rescued by forming the complex with PAI1^{R76E}, by silencing *LRP1* gene expression and by treating cells with RAP.

Upon de-repression, the signaling activity of tPA–PAI1 complex required NMDA-R, similar to what is seen with free tPA. Significant binding of tPA–PAI1 complex to immuno-purified NMDA-R was demonstrated. The extent of binding of tPA–PAI1 complex to immunopurified NMDA-R might be less than that of free tPA; however, this conclusion should be interpreted cautiously

because only one concentration of ligand was studied and immunopurified NMDA-R might behave differently than membrane-anchored NMDA-R.

We considered the possibility, given the high affinity of tPA–PAI1 complex for LRP1 (Stefansson et al., 1998), that signaling by the tPA–PAI1 complex is blocked by LRP1 because LRP1 rapidly clears tPA–PAI1 complex from the cellular microenvironment and thus, prevents binding to NMDA-R. The maximum uptake and degradation of high-affinity ligands by LRP1 in cells with greater than 10^5 copies of LRP1, has been estimated at 50 fmol/10^6 cells per minute (Iadonato et al., 1993; Weaver et al., 1996). In our experiments with nearly confluent cultures of PC12 cells (~0.5×10^6 cells) and 12 nM tPA–PAI1 complex in 2.0 ml medium, 24,000 fmols of tPA–PAI1 complex were present. Applying published ligand uptake rates for LRP1, the concentration of the tPA–PAI1 complex would have been expected to decrease from 12 nM to no lower than 11.9 nM in our ERK1/2 activation experiment. Thus, we do not view depletion of tPA–PAI1 complex from the culture medium as an explanation for the lack of signaling activity by tPA–PAI1 complex. In support of this conclusion, activated α_2M, which binds to LRP1 with high affinity (K_D~1.0 nM) (Weaver et al., 1996; Van Leuven et al., 1979; Hussaini et al., 1990), triggers cell signaling in PC12 cells and SCs when present at a concentration of 10 nM.

Identifying the mechanism by which LRP1 selectively inhibits the cell signaling activity of tPA–PAI1 complex, while promoting cell signaling initiated by free tPA or activated α_2M, will require further investigation. We speculate that binding of tPA–PAI1 complex to LRP1 may sterically hinder the complex from engaging its binding site on the NMDA-R. PAI1-binding to EA-tPA and the resulting high affinity interaction with LRP1 also may inhibit distribution of tPA–PAI1 complex into lipid rafts, where tPA-initiated cell signaling apparently occurs (Laudati et al., 2016).

PAI1 had no effect on the cell signaling activity of EI-tPA or the ability of EI-tPA to stimulate SC migration. This is an important result because tPA has been reported to associate non-covalently with PAI1 through exosite interactions (Ibarra et al., 2004). Apparently, exosite interactions do not trigger PAI1 conformational change, which is required to reveal the cryptic high-affinity LRP1-binding site in PAI1 (Herz et al., 1992; Orth et al., 1992; Stefansson et al., 1998). As a result, the pathway we have uncovered, in which binding of tPA–PAI1 complex to LRP1 inhibits cell signaling initiated by the complex, is not operational.

We hypothesize that the activity of PAI1 observed here, as a regulator of tPA activities mediated by the NMDA-R in PC12 cells, SCs and BMDMs, may be observed in other cells in which tPA binds to the NMDA-R, such as neurons (Nicole et al., 2001; Wu et al., 2013; Yepes, 2015; Chevilley et al., 2015; Lesept et al., 2016; Jeanneret and Yepes, 2017). However, we also recognize that in addition to the NMDA-R, other receptors have been implicated in tPA signaling. One example is Annexin A2 (Siao and Tsirka, 2002; Ortiz-Zapater et al., 2007; Lin et al., 2012; Lin and Hu, 2017). Understanding how PAI1 regulates receptor-mediated activities of tPA, which involve receptors such as Annexin A2, is an important future challenge.

MATERIALS AND METHODS

Proteins and reagents

Human EA-tPA, which is produced in CHO cells and is 95% in the two-chain form, and human EI-tPA, which carries the S478A mutation and is 90% in the single-chain form, were from Molecular Innovations. PAI1, which is mutated to enhance stability and expressed in *Escherichia coli*, gPAI1, which is expressed in insect cells, and PAI1^{R76E} were from Molecular Innovations. Plasminogen was purified from human plasma as previously described (Gonias et al., 1982). Endotoxin-free, monomeric RAP was provided by Dr Travis Stiles (Novoron Biosciences, San Diego, CA). NGFβ was from Invitrogen. LPS serotype 055:B5 from *E. coli* was from Sigma-Aldrich. H-D-Val-Leu-Lys-p-nitroanilide (S-2251) was from Molecular Innovations. Dizocilpine (MK801) was from Cayman Chemicals. Type IV collagen, poly-D-lysine (PDL), AEBSF and fibronectin were from Sigma-Aldrich.

Cell culture model systems

Rat PC12 pheochromocytoma cells were obtained from the ATCC (CRL-1721™) and subjected to quality-control tests by the ATCC. The PC12 cells were cultured in Dulbecco's modified Eagle's medium (DMEM, high glucose; Gibco) containing 10% heat-inactivated fetal bovine serum (FBS; Gibco), 5% heat-inactivated horse serum (Hyclone), penicillin (100 units/ml) and streptomycin (1 mg/ml), in plates coated with 0.01 mg/ml type IV collagen. Cells were passaged no more than eight times.

SCs were isolated from the sciatic nerves of 1-day-old Sprague Dawley rats. The SCs were enriched and separated from fibroblasts using fibronectin-specific antibody and rabbit complement cytolysis. Final preparations consisted of 98% SCs, as determined by immunofluorescence microscopy for S100β, which is a specific SC marker (Mantuano et al., 2015). Primary SC cultures were maintained in plates coated with 1.0 µg/ml PDL in low-glucose DMEM containing 10% FBS, 100 U/ml penicillin, 100 µg/ml streptomycin, 21 µg/ml bovine pituitary extract (Sigma-Aldrich) and 4 µM forskolin (Thermo Scientific), and were passaged no more than six times before conducting experiments.

BMDMs were isolated from the femurs of 16 week old wild-type C57BL/6 mice, as previously described (Mantuano et al., 2016). Bone marrow cells were plated in 100-mm non-tissue culture-treated dishes (10^6 cells/well) and cultured in DMEM/F-12 medium containing 10% FBS and 20% L929 cell-conditioned medium for 10 days. Non-adherent cells were eliminated on day 10. Adherent cells included >95% BMDMs as determined by F4/80 and CD11b immunoreactivity (Mantuano et al., 2016, 2017).

All animal experiments were performed according to approved guidelines.

LRP1 gene silencing in PC12 cells

Rat LRP1-specific siRNA ON-TARGETplus SMARTpool (L-101489-02) and NTC siRNA (D-001810-10) were from Dharmacon. PC12 cells (2×10^6) were transfected with LRP1-specific or NTC siRNA (120 nM) by electroporation using the Cell Line Nucleofector Kit V (Amaxa VCA-1003). The extent of gene silencing was determined with immunoblot analysis using an antibody specific for 85-kDa LRP1 β-chain (1:1000, Abcam, Ab-215997). Immunoblots were subjected to densitometry. Experiments were performed 36-48 h after transfection.

PAI1 activity assay

EA-tPA was incubated with PAI1, gPAI1, PAI1^{R76E} or vehicle in 50 µl of 20 mM sodium phosphate, 150 mM NaCl, pH 7.4 (PBS) for 30 min. EA-tPA was treated with AEBSF for 2 h. Plasminogen and S-2251 were then added so the final volume was 150 µl. The final concentration of EA-tPA (alone or in complex with PAI1) was 12 nM. The concentrations of plasminogen and S-2251 were 0.2 µM and 0.2 mM, respectively. S-2251 hydrolysis was detected by monitoring the absorbance at 405 nm as a function of time using a Spectramax M2 ELISA plate reader.

Analysis of cell signaling

PC12 cells were cultured in serum-containing medium until ~70% confluent. The cells were then transferred to serum-free medium (SFM) for 4 h and treated with EA-tPA, AEBSF-treated EA-tPA, EA-tPA–PAI1 complex, EA-tPA–gPAI1 complex, EA-tPA–PAI1^{R76E} complex or free PAI1 for 10 min. In some studies, PC12 cells were pre-treated with 150 nM RAP or 1.0 µM MK801 for 30 min before adding candidate cell signaling activators. PC12 cells that were transfected with LRP1-specific or NTC siRNA were treated with EA-tPA or EA-tPA–PAI1 complex for 1 h.

SCs that were 70% confluent were transferred to SFM for 1 h and then treated with EA-tPA or the EA-tPA–PAI1 complex for 1 h. BMDMs were transferred to SFM for 30 min and then treated with LPS (0.1 µg/ml) together with EA-tPA, tPA–PAI1 complex, free PAI1 or vehicle for 1 h.

Extracts of PC12 cells, SCs and BMDMs were prepared in RIPA buffer (PBS with 1% Triton X-100, 0.5% sodium deoxycholate, 0.1% SDS, protease inhibitor mixture and phosphatase inhibitor mixture). The protein concentration in cell extracts was determined with a bicinchoninic acid assay. An equivalent amount of cellular protein (20–40 µg) was subjected to 10% SDS-PAGE and electrotransferred to polyvinylidene fluoride membranes. The membranes were blocked with 5% nonfat dried milk and 0.1% Tween 20 and incubated with primary antibodies from Cell Signaling Technology that target: phospho-IκBα (1:1000, cat. 2859), total IκBα (1:1000, 9242), phospho-ERK1/2 (1:2000, 4370), total-ERK1/2 (1:1000, 4695) and β-actin (1:5000, 3700). The membranes were washed and treated with horseradish-peroxidase-conjugated secondary antibodies from Jackson Laboratories (anti-rabbit IgG, 111-035-144; anti-mouse IgG, 15-035-146). Immunoblots were developed using SuperSignal West Pico PLUS substrate (Thermo Scientific) and imaged using Blue Devil autoradiography film (Genesee Scientific) or the Azure Biosystems C300 system.

PC12 cell neurite outgrowth

PC12 cells were plated at 2×10^5 cells/well in six-well plates and maintained in serum-containing medium for 24 h. The medium then was replaced with SFM, and supplemented with tPA, preformed tPA–PAI1 complex, PAI1, NGFβ or vehicle. Culturing was continued for 48 h; the medium and added proteins were replaced after washing at 24 h. Neurite outgrowth was assessed by phase-contrast microscopy using a Leica microscope equipped with a DFC 300 digital camera and quantified using the ImageJ plugin, NeuronJ.

SC migration

SC migration was studied using 6.5-mm Transwell chambers with 8 µm pores (Corning), as previously described (Mantuano et al., 2015, 2008). The bottom surface of each membrane was coated with 10 µg/ml fibronectin. SCs in Sato medium (Bottenstein and Sato, 1980) supplemented with 1 mg/ml BSA were pre-treated with EA-tPA (12 nM), EI-tPA (12 nM), tPA–PAI1 complex (12 nM), free PAI1 (36 nM), EI-tPA that was pre-incubated with PAI1 or vehicle for 10 min at 37°C. The cells (10^4) were then transferred to the upper Transwell chambers. The bottom chamber contained Sato Medium with 1 mg/ml BSA, 10% FBS and the same proteins that were added to the top chamber. Cell migration was allowed to occur for 4 h at 37°C in 5% CO_2. The upper surface of each membrane was cleaned with a cotton swab. The membranes were then stained with PROTOCOL™ Hema 3™. The number of cells on the bottom surface of each membrane was imaged and counted using ImageJ. Five fields were examined on each filter. Each condition was studied in quadruplicate.

RT-qPCR analysis of cytokine expression in BMDMs

BMDMs were transferred to SFM for 30 min and then treated with LPS (0.1 µg/ml), EA-tPA, EA-tPA–PAI1 complex or PAI1, at the indicated concentrations, alone or in combination for 6 h. RNA was isolated using the NucleoSpin RNA kit (Macherey-Nagel) and reverse-transcribed using the iScript cDNA synthesis kit (Bio-Rad). qPCR was performed using TaqMan gene expression products (Thermo Scientific). The mRNAs analyzed included those encoding TNFα, IL-1β, IL-6 and CCL3. The relative change in mRNA expression was calculated using the $2^{\Delta\Delta Ct}$ method with *GAPDH* mRNA as an internal normalizer.

Immunopurification of NMDA-R

C57BL/6 mice were euthanized with CO_2, according to a protocol approved by the University of California San Diego Institutional Animal Care and Use Committee. Cerebral cortices were harvested and then suspended in ice-cold 50 mM Tris-HCl, 150 mM NaCl, 1% NP40, pH. 8.0, supplemented with proteinase inhibitor cocktail (Pierce) (IP buffer) and manually dissociated using Biomasher (Omni) and vortexing. Extracts were cleared by centrifugation at 13,000 ***g*** for 10 min, diluted five-fold in immunoprecipitation bufffer and then pre-cleared by incubation with Protein G–Dynabeads (Thermo Scientific) in the absence of antibodies for 2 h at 4°C.

NMDA-R NR1 subunit-specific antibody (NR1-Ab) (Millipore; 05-432) and non-specific mouse IgG (NS-IgG) were coupled to Protein-G–Dynabeads by incubation for 30 min at 4°C. Antibody–Protein-G–Dynabeads conjugates were stabilized by treatment with 5 mM bis(sulfosuccinimidyl)suberate for 30 min in PBS at room temperature. The crosslinking reaction was quenched with 20 mM Tris-HCl pH 8. Pre-cleared mouse cortical extracts were incubated with the antibody-conjugated Protein G–Dynabeads for 2 h at 4°C. Binding of the NMDA-R to NR1-Ab and NS-IgG was determined by immunoblot analysis. For these studies, antibody-associated proteins were eluted in 100 mM glycine, pH 2.75 at 57°C while shaking in a thermomixer at 800 rpm. The eluent was rapidly neutralized by adding 1.5 M Tris-HCl pH 8.0, and subsequently subjected to SDS-PAGE. Following electro-transfer, membranes were probed with rabbit anti-NR1 antibody (1:500, Cell Signaling Technology, 5704) and detected using a secondary horseradish peroxidase-conjugated antibody that specifically recognizes rabbit IgG light chain (Jackson Laboratories; 115-035-174).

tPA-binding to immunopurified NMDA-R

EA-tPA was radioiodinated by incubation with 18.5 MBq of $Na^{125}I$ and two Iodobeads (Pierce) for 15 min. ^{125}I-EA-tPA was purified from free $Na^{125}I$ by chromatography on Sephadex G25. The specific activity was 22 mCurie/g. ^{125}I-EA-tPA (12 nM) and preformed ^{125}I-EA-tPA–PAI1 complex (12 nM) were incubated with NMDA-R that was immunocaptured by NR1-Ab–Protein G–Dynabeads or with NS-IgG–Protein G–Dynabeads conjugates, which were pre-incubated with mouse cortical extracts as a control. The beads were washed three times with ice-cold PBS. The level of antibody-associated ^{125}I-EA-tPA was determined in a Wizard 1470 Gamma Counter (Perkin Elmer).

Competing interests

The authors declare no competing or financial interests.

Author contributions

Conceptualization: S.L.G., E.M.; Methodology: S.L.G., A.S.G., W.M.C., E.M.; Validation: S.L.G., M.A.B., A.S.G., P.A., W.M.C., E.M.; Formal analysis: S.L.G., M.A.B., A.S.G., P.A., W.M.C., E.M.; Investigation: M.A.B., A.S.G., P.A., E.M.; Writing - original draft: S.L.G., M.A.B., E.M.; Writing - review & editing: S.L.G., M.A.B., A.S.G., P.A., W.M.C., E.M.; Visualization: S.L.G., M.A.B., A.S.G., P.A., W.M.C., E.M.; Supervision: S.L.G., W.M.C., E.M.; Project administration: S.L.G.; Funding acquisition: S.L.G., W.M.C., E.M.

Funding

This work was supported by National Institutes of Health (grant R01 HL136395 to S.L.G., grant R01 NS097590 to S.L.G. and W.M.C.), and by the Ministry of Education, Universities and Research (Italy, grant FIRB 2013 RBFR13RBK9 to E.M.). Deposited in PMC for release after 12 months.

References

Alessi, M. C. and Juhan-Vague, I. (2006). PAI-1 and the metabolic syndrome: links, causes, and consequences. *Arterioscler. Thromb. Vasc. Biol.* **26**, 2200-2207.

Bacskai, B., Xia, M., Strickland, D., Rebeck, G. and Hyman, B. (2000). The endocytic receptor protein LRP also mediates neuronal calcium signaling via N-methyl-D-aspartate receptors. *Proc. Natl. Acad. Sci. USA* **97**, 1155111556.

Bajou, K., Noel, A., Gerard, R. D., Masson, V., Brunner, N., Holst-Hansen, C., Skobe, M., Fusenig, N. E., Carmeliet, P., Collen, D. et al. (1998). Absence of host plasminogen activator inhibitor 1 prevents cancer invasion and vascularization. *Nat. Med.* **4**, 923-928.

Bode, W. and Renatus, M. (1997). Tissue-type plasminogen activator: variants and crystal/solution structures demarcate structural determinants of function. *Curr. Opin. Struct. Biol.* **7**, 865-872.

Bottenstein, J. and Sato, G. (1980). Fibronectin and polylysine requirement for proliferation of neuroblastoma cells in defined medium. *Exp. Cell Res.* **129**, 361-366.

Bu, G., Williams, S., Strickland, D. K. and Schwartz, A. L. (1992). Low density lipoprotein receptor-related protein/alpha 2-macroglobulin receptor is an hepatic receptor for tissue-type plasminogen activator. *Proc. Natl. Acad. Sci. USA* **89**, 7427-7431.

Carmeliet, P., Schoonjans, L., Kieckens, L., Ream, B., Degen, J., Bronson, R., De Vos, R., Van Den Oord, J. J., Collen, D. and Mulligan, R. C. (1994). Physiological consequences of loss of plasminogen activator gene function in mice. *Nature* **368**, 419-424.

Chevilley, A., Lesept, F., Lenoir, S., Ali, C., Parcq, J. and Vivien, D. (2015). Impacts of tissue-type plasminogen activator (tPA) on neuronal survival. *Front. Cell. Neurosci.* **9**, 415.

Collen, D. and Lijnen, H. R. (1991). Basic and clinical aspects of fibrinolysis and thrombolysis. *Blood* **78**, 3114-3124.
Czekay, R., Aertgeerts, K., Curriden, S. and Loskutoff, D. (2003). Plasminogen activator inhibitor-1 detaches cells from extracellular matrices by inactivating integrins. *J. Cell Biol.* **160**, 781-791.
Deng, G., Curriden, S. A., Wang, S., Rosenberg, S. and Loskutoff, D. J. (1996). Is plasminogen activator inhibitor-1 the molecular switch that governs urokinase receptor-mediated cell adhesion and release? *J. Cell Biol.* **134**, 1563-1571.
De Taeye, B., Smith, L. H. and Vaughan, D. E. (2005). Plasminogen activator inhibitor-1: a common denominator in obesity, diabetes and cardiovascular disease. *Curr. Opin. Pharmacol.* **5**, 149-154.
Devaraj, S., Xu, D. Y. and Jialal, I. (2003). C-reactive protein increases plasminogen activator inhibitor-1 expression and activity in human aortic endothelial cells: implications for the metabolic syndrome and atherothrombosis. *Circulation* **107**, 398-404.
Echeverry, R., Wu, J., Haile, W. B., Guzman, J. and Yepes, M. (2010). Tissue-type plasminogen activator is a neuroprotectant in the mouse hippocampus. *J. Clin. Invest.* **120**, 2194-2205.
Ghosh, S. and Karin, M. (2002). Missing pieces in the NF-kappaB puzzle. *Cell* **109** S81-S96.
Gonias, S. L., Einarsson, M. and Pizzo, S. V. (1982). Catabolic pathways for streptokinase, plasmin, and streptokinase activator complex in mice. In vivo reaction of plasminogen activator with alpha 2-macroglobulin. *J. Clin. Invest.* **70**, 412-423.
Hajjar, K. A., Jacovina, A. T. and Chacko, J. (1994). An endothelial cell receptor for plasminogen/tissue plasminogen activator. I. Identity with annexin II. *J. Biol. Chem.* **269**, 21191-21197.
Hall, S. W., Humphries, J. E. and Gonias, S. L. (1991). Inhibition of cell surface receptor-bound plasmin by alpha 2-antiplasmin and alpha 2-macroglobulin. *J. Biol. Chem.* **266**, 12329-12336.
Hekman, C. M. and Loskutoff, D. J. (1988). Kinetic analysis of the interactions between plasminogen activator inhibitor 1 and both urokinase and tissue plasminogen activator. *Arch. Biochem. Biophys.* **262**, 199-210.
Herz, J., Clouthier, D. E. and Hammer, R. E. (1992). LDL receptor-related protein internalizes and degrades uPA-PAI-1 complexes and is essential for embryo implantation. *Cell* **71**, 411-421.
Hoylaerts, M., Rijken, D. C., Lijnen, H. R. and Collen, D. (1982). Kinetics of the activation of plasminogen by human tissue plasminogen activator. Role of fibrin. *J. Biol. Chem.* **257**, 2912-2919.
Hussaini, I. M., Srikumar, K., Quesenberry, P. J. and Gonias, S. L. (1990). Colony-stimulating factor-1 modulates alpha 2-macroglobulin receptor expression in murine bone marrow macrophages. *J. Biol. Chem.* **265**, 19441-19446.
Iadonato, S. P., Bu, G., Maksymovitch, E. A. and Schwartz, A. L. (1993). Interaction of a 39 kDa protein with the low-density-lipoprotein-receptor-related protein (LRP) on rat hepatoma cells. *Biochem. J.* **296**, 867-875.
Ibarra, C. A., Blouse, G. E., Christian, T. D. and Shore, J. D. (2004). The contribution of the exosite residues of plasminogen activator inhibitor-1 to proteinase inhibition. *J. Biol. Chem.* **279**, 3643-3650.
Jeanneret, V. and Yepes, M. (2017). Tissue-type plasminogen activator is a homeostatic regulator of synaptic function in the central nervous system. *Neural Regen. Res.* **12**, 362-365.
Laudati, E., Gilder, A. S., Lam, M. S., Misasi, R., Sorice, M., Gonias, S. L. and Mantuano, E. (2016). The activities of LDL Receptor-related Protein-1 (LRP1) compartmentalize into distinct plasma membrane microdomains. *Mol. Cell. Neurosci.* **76**, 42-51.
Lesept, F., Chevilley, A., Jezequel, J., Ladépêche, L., Macrez, R., Aimable, M., Lenoir, S., Bertrand, T., Rubrecht, L., Galea, P. et al. (2016). Tissue-type plasminogen activator controls neuronal death by raising surface dynamics of extrasynaptic NMDA receptors. *Cell Death Dis.* **7**, e2466.
Lin, L. and Hu, K. (2017). Tissue-type plasminogen activator modulates macrophage M2 to M1 phenotypic change through annexin A2-mediated NF-kappaB pathway. *Oncotarget* **8**, 88094-88103.
Lin, L., Wu, C. and Hu, K. (2012). Tissue plasminogen activator activates NF-kappaB through a pathway involving annexin A2/CD11b and integrin-linked kinase. *J. Am. Soc. Nephrol.* **23**, 1329-1338.
Liot, G., Roussel, B. D., Lebeurrier, N., Benchenane, K., Lopez-Atalaya, J. P., Vivien, D. and Ali, C. (2006). Tissue-type plasminogen activator rescues neurones from serum deprivation-induced apoptosis through a mechanism independent of its proteolytic activity. *J. Neurochem.* **98**, 1458-1464.
Mantuano, E., Inoue, G., Li, X., Takahashi, K., Gaultier, A., Gonias, S. L. and Campana, W. M. (2008). The hemopexin domain of matrix metalloproteinase-9 activates cell signaling and promotes migration of schwann cells by binding to low-density lipoprotein receptor-related protein. *J. Neurosci.* **28**, 11571-11582.
Mantuano, E., Jo, M., Gonias, S. and Campana, W. (2010). Low density lipoprotein receptor-related protein (LRP1) regulates Rac1 and RhoA reciprocally to control Schwann cell adhesion and migration. *J. Biol. Chem.* **285**, 14259-14266.
Mantuano, E., Lam, M. S. and Gonias, S. L. (2013). LRP1 assembles unique co-receptor systems to initiate cell signaling in response to tissue-type plasminogen activator and myelin-associated glycoprotein. *J. Biol. Chem.* **288**, 34009-34018.
Mantuano, E., Lam, M. S., Shibayama, M., Campana, W. M. and Gonias, S. L. (2015). The NMDA receptor functions independently and as an LRP1 co-receptor to promote Schwann cell survival and migration. *J. Cell Sci.* **128**, 3478-3488.
Mantuano, E., Brifault, C., Lam, M. S., Azmoon, P., Gilder, A. S. and Gonias, S. L. (2016). LDL receptor-related protein-1 regulates NFkappaB and microRNA-155 in macrophages to control the inflammatory response. *Proc. Natl. Acad. Sci. USA* **113**, 1369-1374.
Mantuano, E., Azmoon, P., Brifault, C., Banki, M. A., Gilder, A. S., Campana, and W. M., Gonias, S. L. (2017). Tissue-type plasminogen activator regulates macrophage activation and innate immunity. *Blood* **130**, 1364-1374.
Martin, A. M., Kuhlmann, C., Trossbach, S., Jaeger, S., Waldron, E., Roebroek, A., Luhmann, H. J., Laatsch, A., Weggen, S., Lessmann, V. et al. (2008). The functional role of the second NPXY motif of the LRP1 beta-chain in tissue-type plasminogen activator-mediated activation of N-methyl-D-aspartate receptors. *J. Biol. Chem.* **283**, 12004-12013.
May, P., Rohlmann, A., Bock, H. H., Zurhove, K., Marth, J. D., Schomburg, E., D., Noebels, J. L., Beffert, U., Sweatt, J. D., Weeber, E. J. et al. (2004). Neuronal LRP1 functionally associates with postsynaptic proteins and is required for normal motor function in mice. *Mol. Cell. Biol.* **24**, 8872-8883.
Miles, L. A., Lighvani, S., Baik, N., Parmer, C. M., Khaldoyanidi, S., Mueller, B. M. and Parmer, R. J. (2014). New insights into the role of Plg-RKT in macrophage recruitment. *Int. Rev. Cell Mol. Biol.* **309**, 259-302.
Moser, T. L., Enghild, J. J., Pizzo, S. V. and Stack, M. S. (1993). The extracellular matrix proteins laminin and fibronectin contain binding domains for human plasminogen and tissue plasminogen activator. *J. Biol. Chem.* **268**, 18917-18923.
Mosesson, M. W. (2005). Fibrinogen and fibrin structure and functions. *J. Thromb. Haemost.* **3**, 1894-1904.
Nakajima, C., Kulik, A., Frotscher, M., Herz, J., Schafer, M., Bock, H. and May, P. H. (2013). Low density lipoprotein receptor-related protein 1 (LRP1) modulates N-methyl-D-aspartate (NMDA) receptor-dependent intracellular signaling and NMDA-induced regulation of postsynaptic protein complexes. *J. Biol. Chem.* **288**, 21909-21923.
Nassar, T., Bdeir, K., Yarovoi, S., Fanne, R. A., Murciano, J. C., Idell, S., Allen, T. C., Cines, D. B. and Higazi, A. A.-R. (2011). tPA regulates pulmonary vascular activity through NMDA receptors. *Am. J. Physiol. Lung Cell. Mol. Physiol.* **301**, L307-L314.
Nicole, O., Docagne, F., Ali, C., Margaill, I., Carmeliet, P., Mackenzie, E. T., vivien, D. and Buisson, A. (2001). The proteolytic activity of tissue-plasminogen activator enhances NMDA receptor-mediated signaling. *Nat. Med.* **7**, 59-64.
Ny, T., Elgh, F. and Lund, B. (1984). The structure of the human tissue-type plasminogen activator gene: correlation of intron and exon structures to functional and structural domains. *Proc. Natl. Acad. Sci. USA* **81**, 5355-5359.
Orth, K., Madison, E. L., Gething, M. J., Sambrook, J. F. and Herz, J. (1992). Complexes of tissue-type plasminogen activator and its serpin inhibitor plasminogen-activator inhibitor type 1 are internalized by means of the low density lipoprotein receptor-related protein/alpha 2-macroglobulin receptor. *Proc. Natl. Acad. Sci. USA* **89**, 7422-7426.
Ortiz-Zapater, E., Peiro, S., Roda, O., Corominas, J. M., Aguilar, S., Ampurdanes, C., Real, F. X. and Navarro, P. (2007). Tissue plasminogen activator induces pancreatic cancer cell proliferation by a non-catalytic mechanism that requires extracellular signal-regulated kinase 1/2 activation through epidermal growth factor receptor and annexin A2. *Am. J. Pathol.* **170**, 1573-1584.
Parcq, J., Bertrand, T., Baron, A. F., Hommet, Y., Angles-Cano, E. and Vivien, D. (2013). Molecular requirements for safer generation of thrombolytics by bioengineering the tissue-type plasminogen activator A chain. *J. Thromb. Haemost.* **11**, 539-546.
Plow, E. F., Freaney, D. E., Plescia, J. and Miles, L. A. (1986). The plasminogen system and cell surfaces: evidence for plasminogen and urokinase receptors on the same cell type. *J. Cell Biol.* **103**, 2411-2420.
Qiu, Z., Strickland, D. K., Hyman, B. T. and Rebeck, G. W. (2002). alpha 2-Macroglobulin exposure reduces calcium responses to N-methyl-D-aspartate via low density lipoprotein receptor-related protein in cultured hippocampal neurons. *J. Biol. Chem.* **277**, 14458-14466.
Samson, A. L., Nevin, S. T., Croucher, D., Niego, B., Daniel, P. B., Weiss, T. W., Moreno, E., Monard, D., Lawrence, D. A., Medcalf, R. L. (2008). Tissue-type plasminogen activator requires a co-receptor to enhance NMDA receptor function. *J. Neurochem.* **107**, 1091-1101.
Sawdey, M. S. and Loskutoff, D. J. (1991). Regulation of murine type 1 plasminogen activator inhibitor gene expression in vivo. Tissue specificity and induction by lipopolysaccharide, tumor necrosis factor-alpha, and transforming growth factor-beta. *J. Clin. Invest.* **88**, 1346-1353.
Siao, C. J. and Tsirka, S. E. (2002). Tissue plasminogen activator mediates microglial activation via its finger domain through annexin II. *J. Neurosci.* **22**, 3352-3358.
Stefansson, S. and Lawrence, D. A. (1996). The serpin PAI-1 inhibits cell migration by blocking integrin alpha V beta 3 binding to vitronectin. *Nature* **383**, 441-443.
Stefansson, S., Muhammad, S., Cheng, X. F., Battey, F. D., Strickland, D. K. and Lawrence, D. A. (1998). Plasminogen activator inhibitor-1 contains a cryptic high

affinity binding site for the low density lipoprotein receptor-related protein. *J. Biol. Chem.* **273**, 6358-6366.

Uhlen, M., Zhang, C., Lee, S., Sjostedt, E., Fagerberg, L., Bidkhori, G., Benfeitas, R., Arif, M., Liu, Z., Edfors, F. et al. (2017). A pathology atlas of the human cancer transcriptome. *Science* **357**.

Van Leuven, F., Cassiman, J. J. and Van Den Berghe, H. (1979). Demonstration of an alpha2-macroglobulin receptor in human fibroblasts, absent in tumor-derived cell lines. *J. Biol. Chem.* **254**, 5155-5160.

Van Zonneveld, A. J., Veerman, H. and Pannekoek, H. (1986). On the interaction of the finger and the kringle-2 domain of tissue-type plasminogen activator with fibrin. Inhibition of kringle-2 binding to fibrin by epsilon-amino caproic acid. *J. Biol. Chem.* **261**, 14214-14218.

Vaudry, D., Stork, P. J., Lazarovici, P. and Eiden, L. E. (2002). Signaling pathways for PC12 cell differentiation: making the right connections. *Science* **296**, 1648-1649.

Weaver, A. M., Mccabe, M., Kim, I., Allietta, M. M. and Gonias, S. L. (1996). Epidermal growth factor and platelet-derived growth factor-BB induce a stable increase in the activity of low density lipoprotein receptor-related protein in vascular smooth muscle cells by altering receptor distribution and recycling. *J. Biol. Chem.* **271**, 24894-24900.

Webb, D. J., Thomas, K. S. and Gonias, S. L. (2001). Plasminogen activator inhibitor 1 functions as a urokinase response modifier at the level of cell signaling and thereby promotes MCF-7 cell growth. *J. Cell Biol.* **152**, 741-752.

Williams, S. E., Ashcom, J. D., Argraves, W. S. and Strickland, D. K. (1992). A novel mechanism for controlling the activity of alpha 2-macroglobulin receptor/low density lipoprotein receptor-related protein. Multiple regulatory sites for 39-kDa receptor-associated protein. *J. Biol. Chem.* **267**, 9035-9040.

Wu, F., Echeverry, R., Wu, J., An, J., Haile, W. B., Cooper, D. S., Catano, M. and Yepes, M. (2013). Tissue-type plasminogen activator protects neurons from excitotoxin-induced cell death via activation of the ERK1/2-CREB-ATF3 signaling pathway. *Mol. Cell. Neurosci.* **52**, 9-19.

Yepes, M. (2015). Tissue-type plasminogen activator is a neuroprotectant in the central nervous system. *Front. Cell. Neurosci.* **9**, 304.